Iraqi Journal of Natural Sciences and Nanotechnology IJNSN

Magnetic Solid Phase Extraction Based on Multiwalled Carbon Nanotubes for Water Remediation from Bismarck Brown-Y: Isotherm Study

Salah Mahdi Saleh, Ali A. Abdulwahid, Zaki N. Kadhim

Department of Chemistry, College of Science, University of Basra, Basra, Iraq

Corresponding Author: salah.saleh@uobasrah.edu.iq

Keywords:

Adsorption;
Bismarck Brown-Y;
Derivatives Magnetic MWCNTs;
Langmuir model.

Abstract

This study utilized enhanced magnetic derivatives of multi-walled carbon nanotubes, specifically MWCNT-Tris@Fe_3O_4, MWCNT-H@Fe_3O_4, MWCNT-Tetra@Fe_3O_4, and MWCNT-G@Fe_3O_4, to extract and eliminate Bismarck Brown-Y (BB-Y) using the solid phase extraction technique. The solid phases were studied by Fourier Transform Infrared Spectroscopy (FTIR), Field Emission Scanning Electron Microscopy (FESE), Transmission Electron Microscopy (TEM), zeta potential measurement, and X-ray Diffraction (XRD). The optimal extraction conditions were attained with a sorbet weight of 0.01gm and an initial concentration of 600 mg/l of BB-y for every phase. The pH of MWCNT-Tris@Fe3O4 was 6, whereas it was 10 for the other phases. Additionally, the volume of dye utilized in this study was 25 ml. The optimal flow rate for the eluting solvent was determined to be 1.5 mL.min-1 also, this study tested different eluents and their volumes. DMSO was shown to be the most effective eluent, with 2.5 ml giving the highest percentage of recovery. The current study focused on determining adsorption capacity using Langmuir and Freundlich isotherm models under ideal conditions. The Langmuir model showed that the maximum adsorption capacities (qmax) were 1724.138, 1818.182, 1886.793, and 1960.784 mg/g for MWCNT-tris@Fe3O4, MWCNT-H@Fe_3O_4, MWCNT-Tetra@Fe_3O_4, and MWCNT-G@Fe_3O_4, respectively. The study's results indicate that the adsorption of BB-y employing magnetic derivatives of multi-walled carbon nanotubes as an adsorbent is chemisorption.

Introduction

Water contamination by various toxic compounds is currently one of the most pressing global issues. Various dangerous contaminants contaminate the environment due to the rapid increase in human activities, including industrialization, unplanned development, irresponsible utilization of natural

water resources, and significant population expansion [1]. Polluted waters include a diverse range of pollutants, comprising both inorganic and organic substances such as dyes, pesticides, medicines, decomposed organic waste, and organic pollutants. In addition, noxious heavy metals serve as inorganic contaminants [2],[3]. Due to their high color intensity, dyestuffs generally provide excellent coverage even at low concentrations. However, this can lead to undesired color changes in waste materials. These dyes can also hinder sunlight penetration and the consumption of dissolved oxygen, thereby inhibiting the process of photosynthesis. In addition, the discharge of colored textile waste into water increases its mutagenic, carcinogenic, and genotoxic properties, all of which pose significant hazards to the environment and to plant and animal life [4]–[6]. Exposure to Bismarck Brown dye, whether briefly or extended, can result in significant irritation and redness at the site of contact with the eyes and skin. Ingestion of this substance leads to testicular irritation, resulting in symptoms such as nausea, vomiting, diarrhea, discomfort, and redness in the mouth or throat. Failure to halt the activity quickly may result in throat irritation, leading to a constricted chest and bouts of coughing. Consequently, a technique is necessary to diminish the presence of dyes before their discharge into the environment [7].

Various methods are available for removing dyestuffs from wastewater before it is released into the environment. These methods include membrane filtration, coagulation, flocculation, adsorption, modified oxidation processes, photocatalytic degradation, and biological therapy. These methods fall under the three basic techniques of physical, biological, and chemical treatment [8]. Despite dyes' resistance to oxidation, biodegradation, light, and heat, adsorption is still a popular method for their removal because traditional physical approaches, such as adsorption and separating membranes, are the most effective and do not require any additional pretreatment before application. Furthermore, it was regarded as the best and most cost-effective solution[9],[10]. Solid phase extraction SPE is a common method to obtain sufficient samples for analysis. The analyte separation is based on the partition coefficient between the mobile/aqueous phase and the adsorbent. Therefore, the SPE for preconditioning samples has many advantages including quick separation, low solvent consumption, high enrichment efficiency and recovery rate, fast processing, no emulsion generation, and flexibility to use with various detection methods [11][12].

The SPE uses carbon nanoparticles (CNs) such as graphene, graphene oxide, carbon nano-disks, carbon nanotube rings (single or multiwall), and carbon nanocones as adsorbents [13]. Consequently, the CNTs have many features such as purity, surface area, functional groups on the surface, adsorption sites, and experimental settings that affect their adsorption effectiveness, which is

enhanced by their chemical stability, higher surface area, smaller pore size, hollow structure, and ease of modification [14]. Furthermore, the magnetic sorbent with Fe_3O_4, a magnetic nanoparticle (MNP), has attracted the interest of researchers due to its remarkable characteristics. These features include its ability to be efficiently mass-produced through a simple procedure and its large surface area and capacity for adsorption. In addition, Fe_3O_4 has excellent magnetic properties and may be easily separated from its solution utilizing an external magnetic field. Furthermore, it has been identified by its low toxicity [15]. The purpose of this study is to clean water that has been polluted with organic dangerous dye (Bismarck Brown-y) using magnetic solid-phase extraction (SPE) with derivatives of multi-walled carbon nanotubes, Figure 1 referred to Bismarck Brown structure.

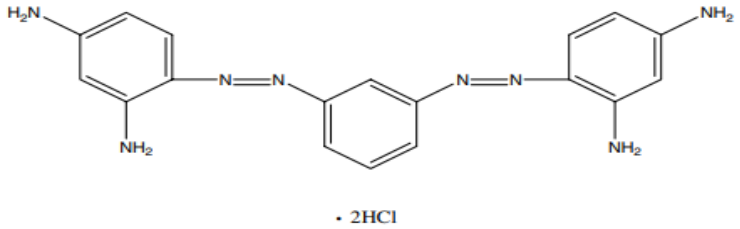

Figure 1 Chemical structure of Bismarck Brown-Y

Experimental procedure

The dyestuff Bismarck-Brown Y, with a chemical formula of C18H20Cl2N8 and a molecular weight of 419.31 g.mol^{-1}, has been purchased from Merck Company. The same manufacturer also supplied the graphite fine powder and DCC (N, N'- Dicyclohexylcarbodiimide). The dye was dissolved in distilled water to make stock solutions, 1000 mg L^{-1}. Two solutions, NaOH (Merck) and HCl (GCC), were used to alter the pH by 0.1 to 0.01 mol. L-1. (Sigma-Aldrich) was the source of the potassium chlorate. The following liquid solvents have been listed by each manufacturer: pure ethanol (formulated by J.T. Baker), absolute methanol (HI media), and dimethylformamide (HI media). A variety of analytical methods were employed to detect MWCNTs, their derivatives, and Fe3O4 decoration, including FT-IR, XRD, TEM, and SEM. The BB-Y dye solution's absorbance was measured at 455.5 nm using a UV-visible spectrophotometer (PG Instrument T80 + UV/VIS). The dye removal efficiency, R, represented as a percentage, and the amount of BB-y dye adsorbed per unit weight of adsorbent at a particular time, q (mg g-1), was calculated as follows.

Recovery%= (Concentration of dye recovery on extraction/ original concentration) *100 (1)

$q= ((C_o-C_e) *V)/M$ (2)

Where, C_e is the BB-Y concentration in milligrams per liter at temperature T, and C_0 is the initial concentration. V is the dye's volume in liters, and M is the solid phase's weight in grams.

Preparation of Multi-Walled Carbon Nanotube.

The current investigation synthesized multi-walled carbon nanotubes (MWCNTs) using a modified version of the Staudenmaier method. The powder of graphite was added to the mixture at a mass-to-volume ratio of 1:10:5 with stirring, the mixture included a concentration of H_2SO_4 and fuming HNO_3, and it was stirred for 30 minutes. After that, the liquid was cooled to 5°C in an ice bath while being agitated vigorously, then gradually added to it $KClO_3$ at a rate of 5:1 (mass: mass). then raise the temperature to solution reached 75°C, and left to sit overnight. The mixture was left to settle in dry air for three days. At the base, a considerable quantity of graphite is deposited. However, some of the reacting carbons kept on to float. Following their collection, one liter of deionized water was added to the carbon particles utilizing a vigorous hour-long stirring process. The solution then headed through a filtration and drying process[16]. Figure 2. Illustrated the steps of synthesis MWCNTs from graphite powder.

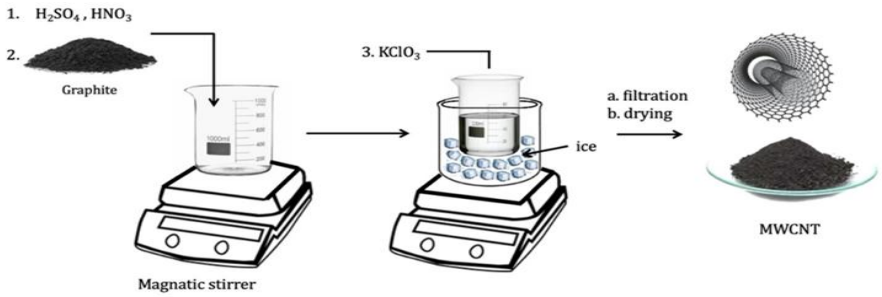

Figure 2 . illustrated the steps of the Synthesis of MWCNTs from Graphite Powder

Purification of MWCNTs.

A 0.05 g impure MWCNT sample was heated by oven to 350 C^o for two hours. This technique removed catalyst contaminants and amorphous carbon. Let the heat-treated MWCNTs cool at ambient temperature. After cooling, MWCNTs were ultrasonically for four hours in 20 milliliters of strong HCl, and then many rinses were done until the pH of the MWCNTs was neutralized. Finally, MWCNTs were dried in an air oven at 100 C^o [17].

Functionalization of MWCNTs.

Chemical oxidation uses nitric and sulfuric acids. 0.1g of pristine multi-walled carbon nanotubes (MWCNTs) were added to a 20-ml combination of 4.0 M nitric acid and 10.0 M sulfuric acid. The

mixture's nitric acid-sulfuric acid ratio was 1:3 to protect the nanotubes. The solution was magnetically stirred for 18 hours at room temperature. Oxidized multi-walled carbon nanotubes (MWCNTs) were purified by separating residual acids. After multiple distilled water washes, the solutions are filtered to a pH of roughly 6. After purification, oxidized samples are dried at 80 degrees Celsius for 12 hours [18].

Modification of MCNT-COOH with Amino Compound.

Multi-walled carbon nanotubes (MWCNTs) generate amide groups when carboxyl groups interact with amine groups. In a 100ml beaker, 1g of MWCMT-COOH was added, followed by 1g of DCC diluted in 20 ml of DMF solvent. Mixtures were stirred at room temperature for 30 minutes. After adding 1.00 g of 4, 4'-Methylenedianiline, tris-(hydroxymethyl) aminomethane, tetraethylenepentamine, or 2, 6-diamine pyridine, a 60 ml methanolic solution was added. With constant agitation, the solution is kept at 60°C for 24 hours. For separation, the mixture was centrifuged at 2500 rpm, washed with DMF-Methanol solution, and rinsed with deionized water. The black precipitate was obtained after drying at 70°C for 10 hours [19].

Decoration of Four Surfaces with Fe_3O_4 as the Magnetic Solid.

Initial iron oxide nanoparticle synthesis used chemical co-precipitation to prepare Fe3O4 magnetic nanoparticles. In summary, 8 mmol (1.5899 g) of $FeCl_2 \cdot 4H_2O$ and 16 mmol (4.32312 g) of $FeCl_3 \cdot 6H_2O$ were dissolved in deionized water in a 100 ml round flask under nitrogen gas and constant stirring. The solution was then heated to 60° C. In 2h, 0.5 mol. L-NH_4OH solution was added to reach pH 9-11. The solution will turn brown, dark brown, then black. With steady stirring, the precipitate cooled to ambient temperature after 30 minutes of constant heating (90 C^o). After multiple rinses with a 1:1 mixture of ethanol and deionized water, the precipitated magnetic nanoparticles were ultra-sonicated for 30 minutes and dried overnight at 60 C^o [20][21]. Thus, 0.5 grams of purified MWCNT/G, MWCNT-Tetra, MWCNT-Tris, or MWCNT-H and 0.125 grams of Fe_3O_4 nanoparticles were individually distributed in 80 milliliters of 1:1 deionized water and ethanol. Thus, the combination was ultrasonicated for 1 hour and then agitated at room temperature for 96 hours. The solution was filtered from the residue using a 200 nm filter. The filtrate was vacuum-dried at 50 C^o for 16 hours [15][21].

Solid Phase Extraction.

The solid phase extraction method required column preparation, loading, and elution[22][23]. Figure 3**.** shown in this work used a polypropylene injection tube as a column (cartridge). A one-mm

polypropylene permeable film (disc) and four glass filter paper sheets lined the column. In this investigation, the column was filled with MWCNT/G@Fe_3O_4, MWCNT/Tris@Fe_3O_4, MWCNT/Tetra@Fe_3O_4, or MWCNT/H@Fe_3O_4. Packed solid phase surfaces should be uniform, level, and equal height. The phase was activated and air space was removed by passing 10 ml of ionic water through the column as the final step. In contrast, the neutral pHpzc dye solution under study was loaded in the second stage.

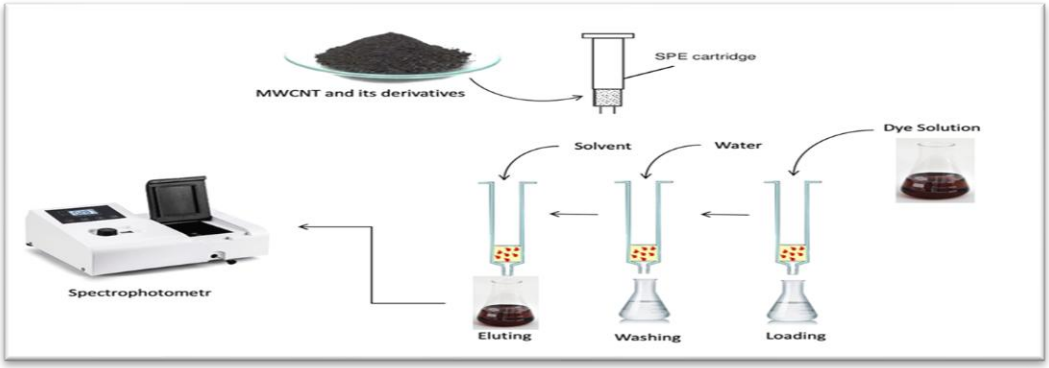

Figure 3 illustrates Using Magnetic MWCNT Derivatives in the Solid Phase Extraction method

Magnetic MWCNT Derivatives Characterization.

Different analytical approaches were used to evaluate the surface features of multi-walled carbon Magnetic MWCNT Derivatives, including FTIR, XRD, FESEM, TEM, and zeta potential analysis. Table 1. for Fourier Transform Infrared (FT-IR) spectroscopy was used to characterize the functional groups in the synthesized solid phases. Include these functional categories to increase diversity and improve extraction. Figure 4 for XRD pattern for characterized of crystallization of compounds. Figure 5, Figure 6 and Table 2 for FESEM and TEM to determine the morphological characterizations of Magnetic MWCNT Derivative, respectively. And Table 3 for zeta potential analysis.

Table 1 FT-IR Spectra for Magnetic MWCNT Derivatives

Compounds	Functional groups (cm^{-1})							
	OH	NH	CH2	C=C	C=O	C-O	C-N	Fe-O
Pre-$MWCNT_S$	-	-	-	1562	-	-	-	-
MWCNT-COOH	3446	-	2899	1564	1672	1082	-	-
MWCNTs-Tris@Fe_3O_4	3543	3441-3491	2947-2991	1583	1718	1093	1163	572

MWCNT-Hetro@Fe_3O_4	-	3414-3475	2828-2910	1514	1622	1091	1240	598
MWCNT-tera@Fe_3O_4	-	3412-3471	2883-2962	1516	1625	1099	1202	596
MWCNT-G@Fe_3O_4	-	3400-3466	3109	1515	1620	=	1251	582

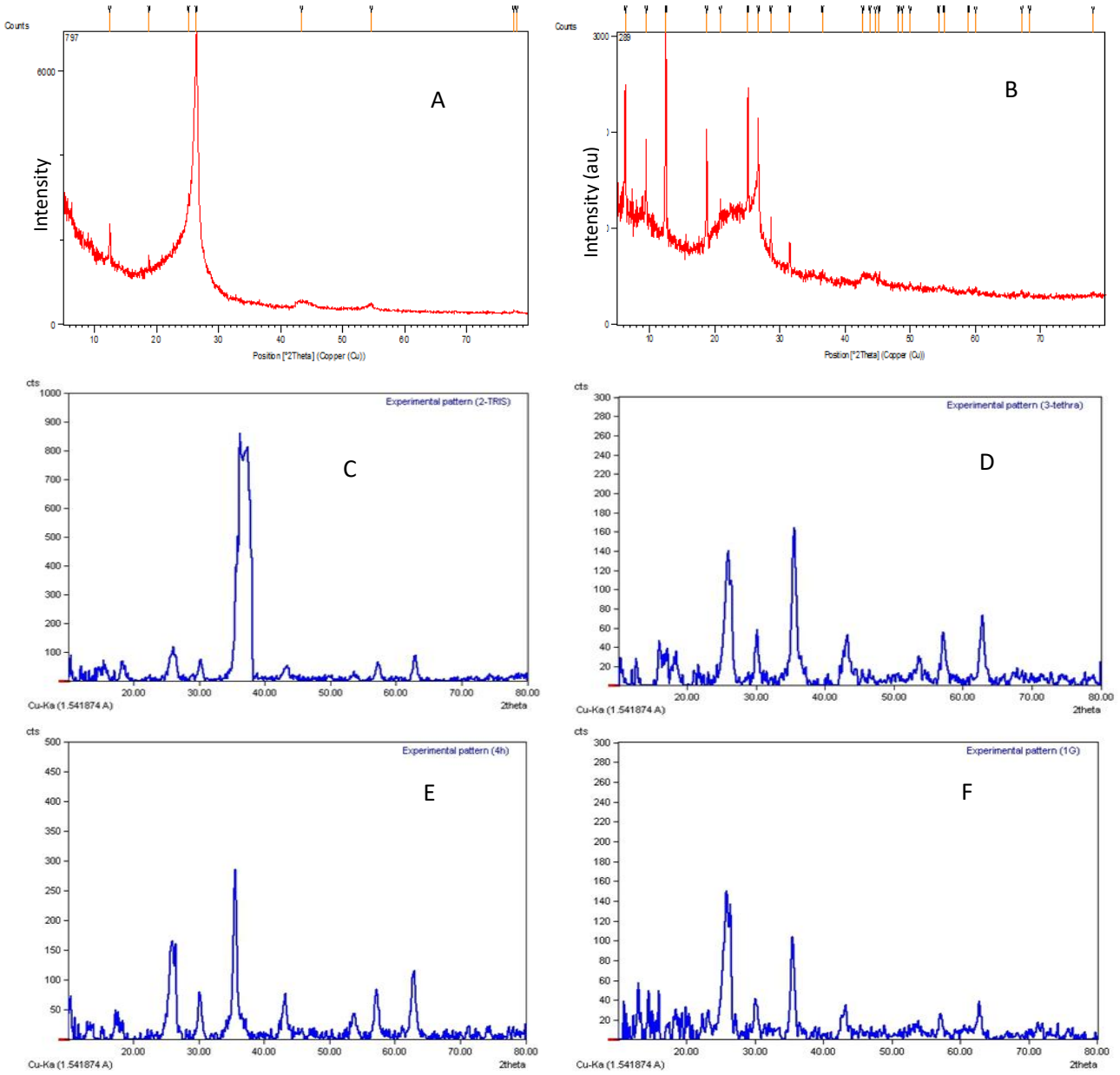

Figure 4 Shown X-ray Diffraction for (A) Prepared MWCNTs (B) Modified MWCNTs with COOH (C) MWCNT-Tris@Fe3O4 (D) MWCNT-Terta@Fe3O4 (E) MWCNT-H@Fe3O4 (F) MWCNT-G@Fe3O4

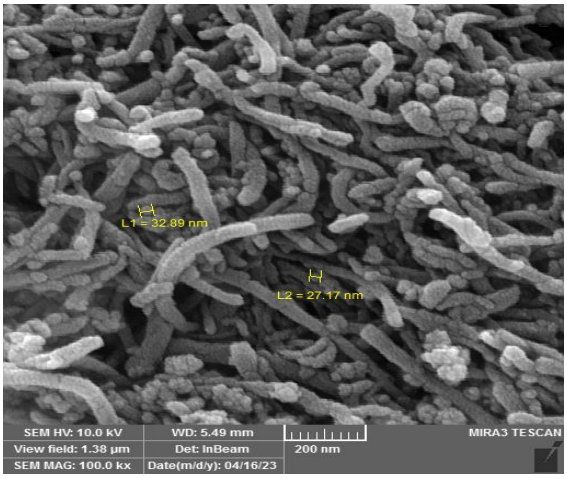

FE-SEM for MWCNTs-Tris@Fe_3O_4

FE-SEM for MWCNTs-Tetra@Fe_3O_4

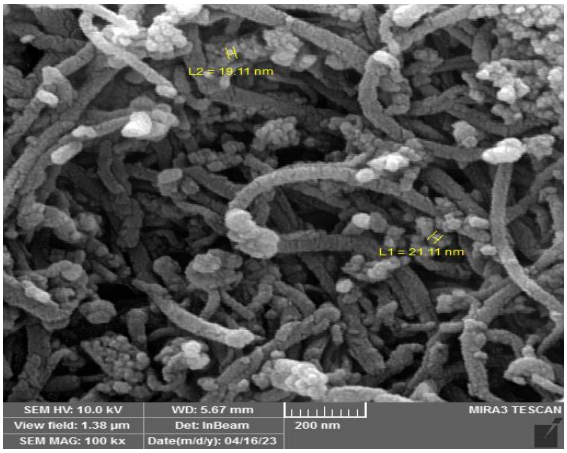

FE-SEM for MWCNTs-Hetro@Fe_3O_4

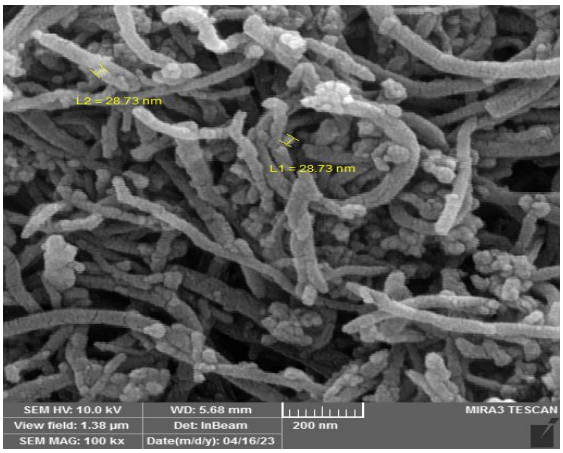

FE-SEM for MWCNTs-G@Fe_3O_4

Figure 5 FE-SEM for MWCNTs-Tris@Fe3O4, MWCNTs-Terta@Fe3O4, MWCNTs-Hetro, Fe3O4 and MWCNTs-G@Fe3O4

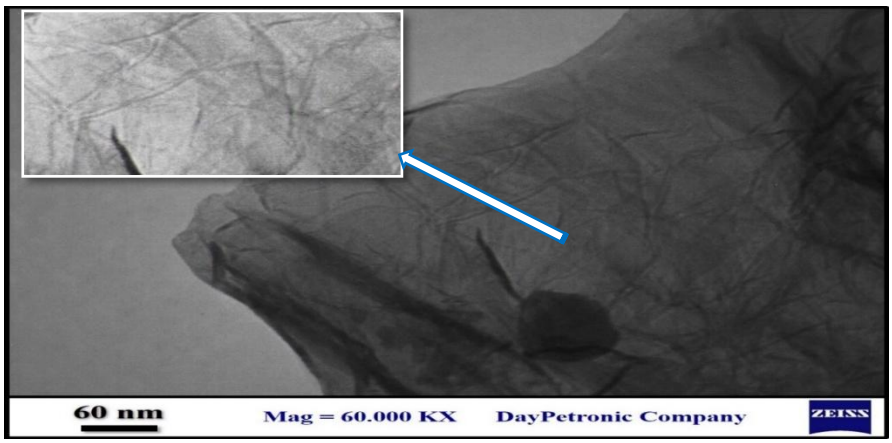

Figure 6 The TEM for Prepared MWCNTs

Table 2 Diameter of prepared MWCNTs

Diameter for MWCNTs(nm)	Minimum	Maximum	Mean
	3.224	8.769	5.847

Table 3 Zeta Potential Values of Magnetic Derivative of MWCNTs

Compound	Zeta-Potential(mV)
MWCNT- Tris @Fe_3O_4	-52.3
MWCNTs-Tetra @Fe3O4	-35.7
MWCNTs-Hetro @ Fe_3O_4	-56
MWCNTs- G@Fe_3O_4	-56.7

Results and discussion:

Optimization of the extraction procedure.

Amount of solid phase.

A certain amount of prepared MWCNT-Tris@ Fe_3O_4, MWCNT-Tetra@ Fe_3O_4, MWCNT-H@ Fe_3O_4, and MWCNT-G@ Fe_3O_4, were weighted as solid phase in separation columns at 5-50 mg. The standard procedure requires beyond conditions. It contains 250 milligrams of dye. L-1, pH 4.2, dye volume 25 ml, flow rate 1ml.min-1, and elution ethanol 10 ml. Figure 7. showed that increasing solid phase weight increases retrieval %, with the maximum value at 0.01g. After stabilizing in the largest weights, the recovery percentages dropped to 0.5g, a trend that was continuous across all solid phases of the BB-y dye study. Thus, the following tests used a solid phase weight of 0.01 g as the standard weight for all phases.

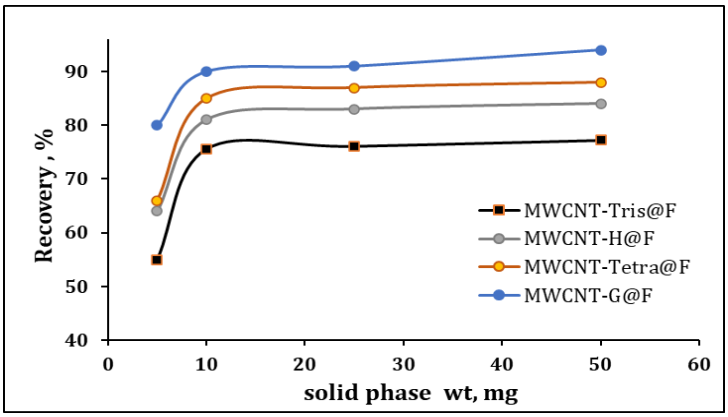

Figure 7 Effect Amount of Magnetic Solid Phase for BB-Y

Effect of Dye Concentration.

The effect of BB-Y dye solution concentrations (50-700) mg/L from the day on 0.01 g of manufactured solid phase (MWCNT-Tris@ Fe_3O4, MWCNT-Tetra@ Fe_3O_4, MWCNT-H@ Fe_3O_4, and MWCNT-G@ Fe_3O_4) was investigated. All other experimental parameters, such as pH, dye volume, flow rate, and elution solution type and volume, were kept constant, as stated in the general procedure, where dye solution concentrations were 600 mg. L^{-1} for all solid phases as Illustrated in Figure 8.

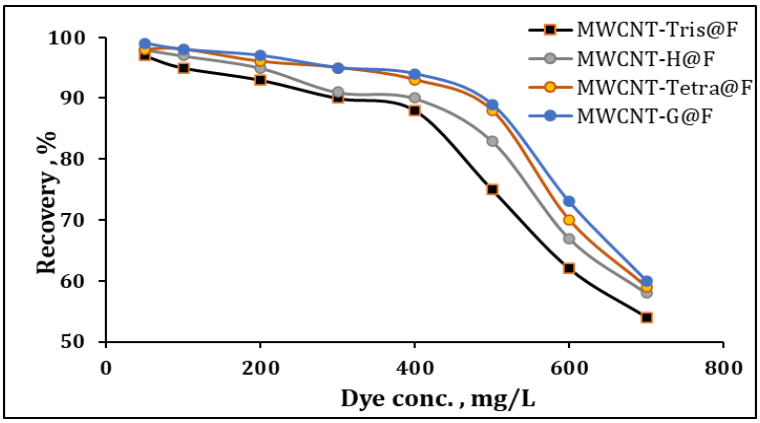

Figure 8 Effect of Bismarck Brown-Y Concentration on the Recovery Percentage

Effect of pH.

Although it directly impacts the solid phase's surface charge and chemical composition, pH is crucial for extraction processes[24]. A study of pH on solid phase extraction was examined from 2-12. Figure 9. shown that MWCNT-Tris@ Fe_3O4enhances cationic dye (BB-y) recovery at pH=6. However, the pH=10 for MWCNT-Tetra@ Fe_3O_4, MWCNT-H@ Fe_3O_4, and MWCNT-G@ Fe_3O_4 respectively. The MWCNTs-Tris contains three hydroxyl groups that increase the negative charge at pH 6. Additionally, the zeta potential is -36 mV, as indicated in Table 3. Protonating the dye results in a positive charge on the nitrogen atom, leading to enhanced adsorption capacity and recovery ratio at pH 6 for MWCNTs-Tris@Fe_3O_4.

$$\text{Dye-NH}_2 + H^+ \longrightarrow \text{Dye-NH}_3^+ \qquad (3)$$

Whenever the pH exceeds 6, the dye solution turns basic, causing deprotonation of the nitrogen atom, resulting in the MWCNTs-Tris@Fe_3O_4 being more negatively charged according to the following equation.

$$–CH_2OH + OH^- \longrightarrow CH_2O^- + H_2O \quad (4)$$

Therefore, the recovery percentage and adsorption capacity decrease as the pH exceeds 6 because of increased repulsion [25][26]. However, the rates of recovery for the three surfaces, MWCNT-Tetra@ Fe_3O_4, MWCNT-H@ Fe_3O_4, and MWCNT-G@ Fe_3O_4, are rising at pH 10, possibly indicating an increase at higher pH levels. The functional groups, such as N–H and C–H groups, on the surfaces mentioned, may function as activation agents due to their negative charges, as seen in Table 3 for zeta potential. As a result, it raised the number of negatively charged molecules. Hence, the adsorption of BB-Y dye may be attributed to the strong electrostatic interaction between the charge on the three surfaces and the positively charged BB-Y molecules [27].

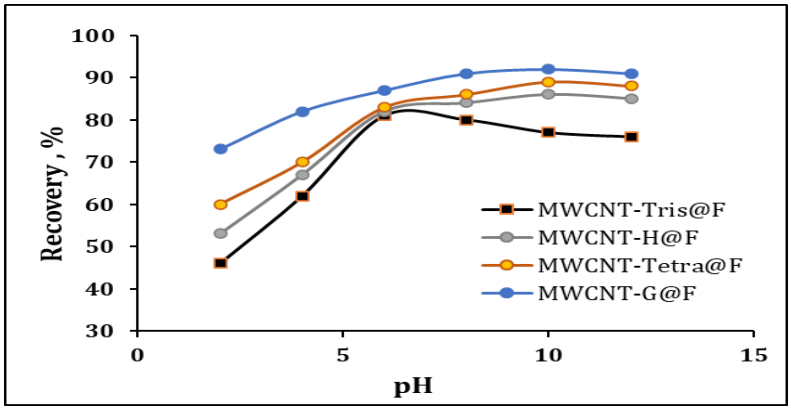

Figure 9 Effect of pH on percentage Recovery of Bismarck Brown-Y

Effect of Dye Volume:

Studying how the solution volume effects on the solid-phase extraction process, especially concerning the target material, is essential for determining the optimal conditions [28][29]. This study investigated various volumes of dye (1ml, 5ml, 10ml, 25ml, 50ml, and 75ml) under the ideal conditions determined by prior tests (0.01g) from all magnetic solid phases at dye concentration 600 mg. L^{-1} and pH 6 for MWCNTs-Tris@Fe_3O_4 and pH 10 for MWCNT-Tetra@ Fe_3O_4, MWCNT-H@ Fe_3O_4, and MWCNT-G@ Fe_3O_4 respectively, with remaining others conditions as mentioned in general method. The recovery percentage as stated in Figure 10. decreased progressively as the volume increased. The observed pattern is due to an obvious relationship between the extraction efficacy and the volume of the solution. As the solution volume grows, the dye concentration decreases, leading to a reduction in extraction efficiency. As the volume of the solution increases, the

dye will dilute at a fundamental level. Hence, the ideal volume is 25ml for the cationic dye Bismarck Brown -Y.

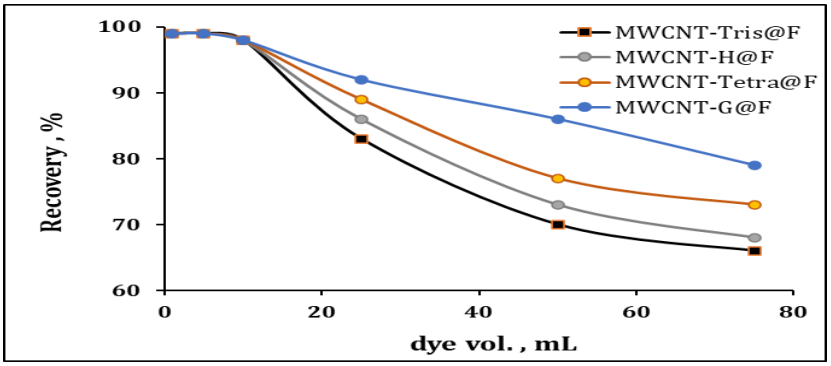

Figure 10 Effect of Bismarck Brown-Y solution volume on the recovery percentage

Effect of Flow Rate:

The flow rate of the dye solution significantly impacts extraction efficiency by ensuring equilibrium in the solid phase [30]. Therefore, Figure 11. illustrated the effect of flow rate, which was investigated in this study form (0.25-2) ml/min, where the optimal flow rate was 1.5 ml per minute. It is worth noting that low flow rate does not take a sufficient time to achieve the equilibrium between the mobile phase (solution of dye) and the stationary phases (surfaces magnetic derivative MWCNTs. Consequently, this factor has significant in SPE method [31][32].

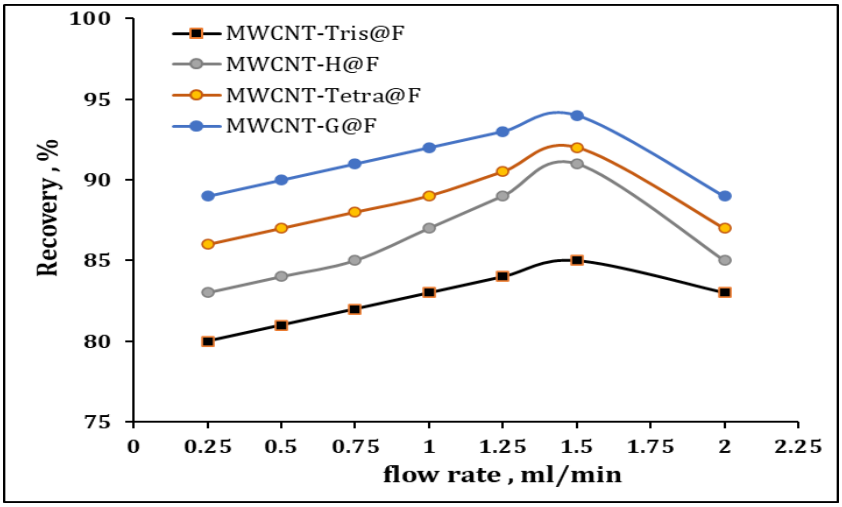

Figure 11 Effect of the Flow Rate of BB-Y Dye Solution on the Magnetic Solid Phase

Effect of Type and Volume of Eluting Solution

This study examines the effects of numerous polar solvents as eluent solvents. The polarity coefficient shows how well the solvent interacts with the solute [33]. As illustrated in Table 4. the solvent polarity of each solvent investigated in this study.

Table 4 Polarity Coefficient and the Solvents used as eluent solution [33]

Solvent	Polarity
DMSO	7.2
Methanol	5.1
Ethanol	4.3
Toluene	2.4
n-Hexane	0.1

Figure 12. Demonstrated the impact of solvent type on R%. The DMSO solvent is the ideal choice because of its greater polarity, which enhances its capacity to separate the adsorbate from the adsorbent. Conversely, the R% diminishes as the polarity of other solvent types decreases, as seen in Table 5. The effect of varied elution solvent volumes on cationic dye separation was also examined. Figure 13. showed that 2.5 ml of DMSO has the greatest effect on dye disengagement. Consequently, the figure showed the appropriate elution solvent volume and percentage recovery correlation. In addition, the enrichment factor studied as shown in Table 4. under study, was consistent and could be used to estimate the optimal elution solvent amount [34].

Enrichment Factor EF= (original dye volume)/ (Elution Volume) (5)

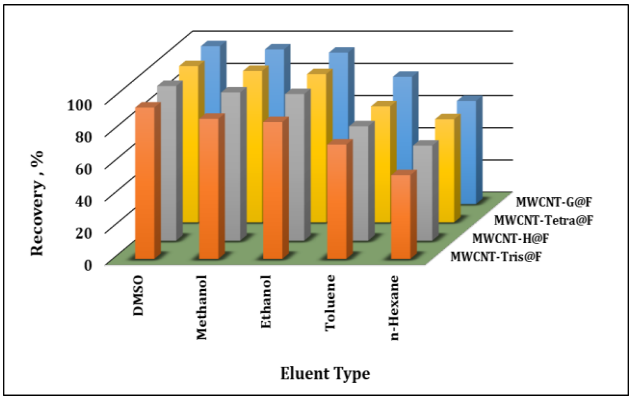

Figure 12. Effect of the Type of Solvent Used as Eluent Solution on BB-Y Dve Extraction

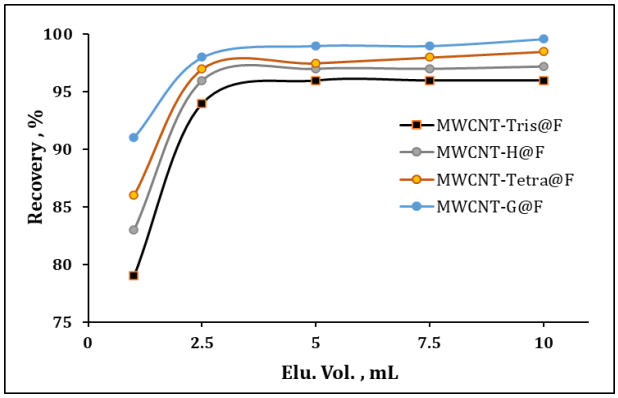

Figure 13. Effect of the Volume Solvent Used as Elution Solvent in BB-Y Dve Extraction

Table 5 Enrichment Factors of Extraction Process BB-Y Dye with Magnetic MWCNT Derivatives@Fe3O4

	Compounds	EF
Bismarck Brown-Y dye	MWCNT-Tris@Fe_3O_4	10
	MWCNT-H@Fe_3O_4	10
	MWCNT-Tetra@Fe_3O_4	10
	MWCNT-G@Fe_3O_4	10

Isotherm Study

SPE is preferred because it is user-friendly, can readily remove unwanted matrix components, and achieves high enrichment factors [35]. Under optimum experimental conditions, BB-Y solutions of particular concentrations were used for adsorption isotherm investigations. The following equation calculated qe (mg/g) adsorption capacity.

$$q_e=((C_o-C_e)\ V)/M \qquad (6)$$

V is the volume of BB-Y dye in liters, and M is the weight of the solid phase extraction surface. The Co (mg/L) and C_e (mg/L) represent the initial and final concentrations of BB-Dye, respectively. Through examining the isotherm, researchers can clarify the relationship between the solid phases and dye, and propose the fundamental mechanisms of interaction [36]. The study utilized the Langmuir model and the Freundlich model to elucidate the behavior of adsorption isotherms.

Langmuir Isotherm Model:

The Langmuir model is founded on the concept of maximum adsorption, where a saturated monolayer of adsorbate (liquid molecules) is formed on the adsorbent (solid surface). The equation is labeled as "Equation 7". This equation presupposes the existence of homogenous adsorption sets [37]. Figure 14**.** displays the Langmuir Isotherm of Adsorption of BB-Y dye in the study.

$$C_o/q_e = \ 1/\ (q_{max}\ X\ K_L) + \ C_o/q_{max} \qquad (7)$$

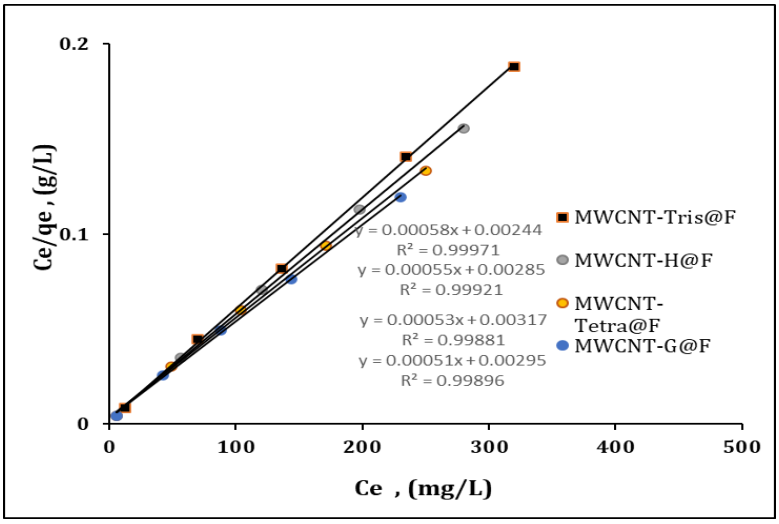

Figure 14. Shown Langmuir Isotherm of Adsorption BB-Y Dye

Figure 14. displayed the Langmuir model for BB-Y, with ($1/q_{max}$) representing the slope of the line. The cutoff is shown as the inverse of q_{max} multiplied by K_L. Using a diagram of the Langmuir equation, the maximum adsorption capacity (q_{max}), Langmuir constant (K_L), and correlation coefficient (R^2) values were determined. The isotherm parameter values for the maximum adsorption capacity of BB-Y dye on four surfaces in the investigation were ranked as follows: MWCNTs-G@Fe_3O_4 < MWCNTs-Tetra@Fe_3O_4 < MWCNTs- Hetro@Fe_3O_4< MWCNTS-Tris@Fe_3O_4. This ranking might be attributed to the increase in surface area achieved by grafting with ferric oxide, as shown in Table 6.

Table 6 Langmuir Isotherm Parameters for Adsorption BB-Y

Solid phases	q_{max}	K_L	R^2
MWCNT-Tris@Fe_3O_4	1724.138	0.238	0.9997
MWCNT-H@Fe_3O_4	1818.182	0.193	0.9992
MWCNT-Tetra@Fe_3O_4	1886.793	0.1672	0.9988
MWCNT-G@Fe_3O_4	1960.784	0.173	0.9989

Freundlich Isotherm Model

The assumption that adsorption occurs at active sets with various adsorption energies allows the equation to explain the phenomena of adsorption and interference on non-homogeneous surfaces. Solute adsorption onto solid surfaces can be better understood with the use of the Freundlich equation, a mathematical model.

$$\ln q_e = \ln K_F + 1/n \ln C_e \quad \ldots\ldots\ldots\ldots\ldots\ldots (8)$$

The Freundlich constant K_F and correlation coefficient R^2 were calculated by plotting the Freundlich equation with lnqe on the Y-axis and lnCe on the X-axis, as shown in Figure 15.

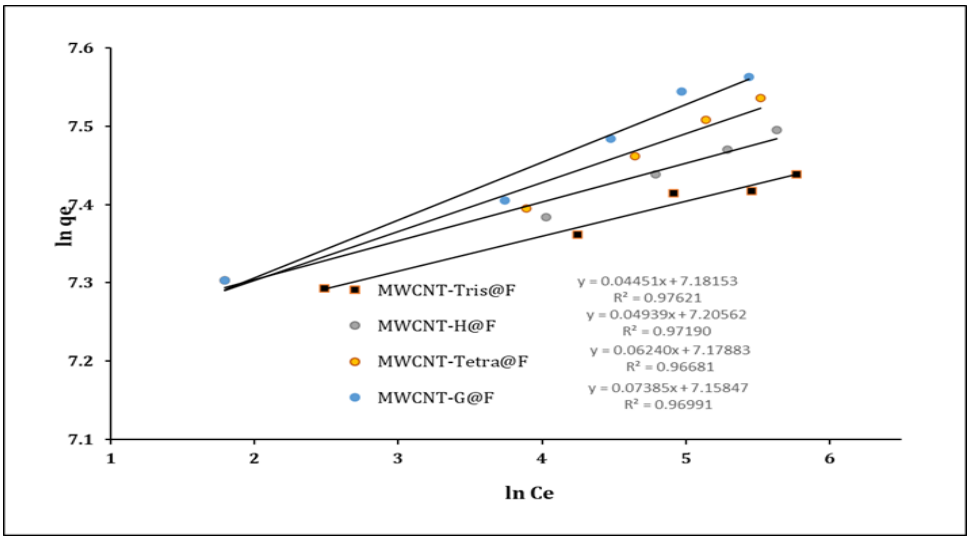

Figure 15. Shown Freundlich Isotherm of Adsorption BB-Y dye

The slope of the straight line varies in direct proportion to 1/n, as seen in Table 6. The cutoff refers to the natural logarithm of the equilibrium constant ($\ln K_F$). The greatest K_F value is found in MWCNT-H@Fe_3O_4, showing the strongest adsorption energy with BB-Y [38] compared to MWCNT-Tris@Fe_3O_4, MWCNT-Tetra@Fe_3O_4, and MWCNT-G@Fe_3O_4, as shown in Table 6. The values of 1/n provide insights into whether the adsorption process is desirable or undesirable. An equilibrium constant of 1/n = 0 indicates irreversible adsorption, while a value between 0 and 1 indicates favorable adsorption between the solid phase and the target substance. If the value of 1/n is bigger than 1, adsorption may not be worthwhile[39][40]. Therefore, Table. 7 displays that the values of 1/n for all magnetic solid phases produced fall between zero and one, suggesting a tendency for adsorption on all surfaces. The R^2 values for the Langmuir and Freundlich models, as shown in

Tables 6 and 7, indicate agreement with the Langmuir equation. Hence, the adsorption mechanism is chemisorption [41].

Table 7 Freundlich Isotherm Parameters for Adsorption BB-Y Dye

Solid phases	1/n	K	R2
MWCNT-Tris@Fe_3O_4	0.04451	1314.919	0.97621
MWCNT-H@Fe_3O_4	0.04939	1346.981	0.9719
MWCNT-Tetra@Fe_3O_4	0.0624	1311.373	0.96681
MWCNT-G@Fe_3O_4	0.07385	1284.944	0.96991

Conclusion:

A magnetic derivative of multi-walled carbon nanotubes (MWCNTs) adsorbent was produced from graphite using four amino acids and transformed into a magnetic material for solid phase extraction. The ideal conditions for Bismarck Brown-Y (BB-Y) dye adsorption using various nano adsorbents such as MWCNTs-Tris@Fe3O4, MWCNTs-H@Fe3O4, MWCNTs-Tetra@Fe3O4, or MWCMTs-G@Fe3O4. An adsorbent dosage of 0.01 g and a dye concentration of 600 mg/L resulted in successful dye removal when using an optimal dye volume of 25 ml. The ideal pH for MWCNTs-Tris@Fe_3O4 was 6, whereas the pH for the other phases was 10. The study examined the flow rate, type, and volume of eluent, which were 1.5 ml/min, DMSO, and 2.5 ml correspondingly. The research paper analyzed two isotherm models, specifically Freundlich and Langmuir. The investigation showed a significant correlation with the Langmuir model, indicated by the high correlation coefficient.

References

[1] N. Ferronato and V. Torretta, "Gelişmekte Olan Ülkelerde Kötü Atık Yönetimi: Küresel Sorunlara Bir Bakış - Waste mismanagement in developing countries: A review of global issues," *International Journal of Environmental Research and Public Health*, vol. 16, no. 6. 2019.

[2] L. Schweitzer and J. Noblet, "Water Contamination and Pollution," in *Green Chemistry*, 2018, pp. 261–290.

[3] J. C. G. Sousa, A. R. Ribeiro, M. O. Barbosa, M. F. R. Pereira, and A. M. T. Silva, "A review on environmental monitoring of water organic pollutants identified by EU guidelines," *J. Hazard. Mater.*, vol. 344, pp. 146–162, 2018.

[4] F. Mcyotto, Q. Wei, D. K. Macharia, M. Huang, C. Shen, and C. W. K. Chow, "Effect of dye structure on color removal efficiency by coagulation," *Chem. Eng. J.*, vol. 405, 2021.

[5] Q. Wei, F. O. Mcyotto, C. W. K. Chow, Z. Nadeem, Z. Li, and J. Liu, "Eco-friendly decolorization of cationic dyes by coagulation using natural coagulant Bentonite and biodegradable flocculant Sodium Alginate," *SDRP J. Earth Sci. Environ. Stud.*, vol. 5, no. 2, pp. 51–60, 2020.

[6] P. Arulmathi, C. Jeyaprabha, P. Sivasankar, and V. Rajkumar, "Treatment of Textile Wastewater by Coagulation–Flocculation Process Using Gossypium herbaceum and Polyaniline Coagulants," *Clean - Soil, Air, Water*, vol. 47, no. 7. 2019.

[7] M. Zakir *et al.*, "Adsroption of Bismarck Brown R Dyes Using Mesoporous Silica MCM-48," *Indones. J. Chem. Res.*, vol. 10, pp. 117–124, 2022.

[8] V. K. K. Gupta and Suhas, "Application of low-cost adsorbents for dye removal – A review," *J. Environ. Manage.*, vol. 90, no. 8, pp. 2313–2342, 2009.

[9] M. Rezaei and A. Habibi-Yangjeh, "Simple and large scale refluxing method for preparation of Ce-doped ZnO nanostructures as highly efficient photocatalyst," *Applied Surface Science*, vol. 265. pp. 591–596, 2013.

[10] B. Mu and A. Wang, "Adsorption of dyes onto palygorskite and its composites: A review," *Journal of Environmental Chemical Engineering*, vol. 4, no. 1. Elsevier Ltd, pp. 1274–1294, Mar. 2016.

[11] X. Hou, S. Tang, and J. Wang "Recent advances and applications of graphene-based extraction." *Trends in Analytical Chemistry,* 2019. doi: .https://doi.org/10.1016/j.trac.2019.07.014.

[12] E. Dziurkowska and M. Wesolowski, "Solid phase extraction purification of saliva samples for antipsychotic drug quantitation," *Molecules*, vol. 23, no. 11, 2018.

[13] R. Bensghaier, I. Tlili, L. Latrou, and A. Megriche, "A New Date Stone Biochar for Efective Solid Phase Extraction of Non-steroidal Anti-infammatory Drugs in Water," *Chem. Africa*, pp. 1–14, 2022.

[14] J. Ben Attig, L. Latrous, M. Zougagh, and Á. Ríos, "Ionic liquid and magnetic multiwalled carbon nanotubes for extraction of N-methylcarbamate pesticides from water samples prior their determination by capillary electrophoresis," *Talanta*, vol. 226. 2021.

[15] A. A. Ensafi, S. Rabiei, B. Rezaei, and A. R. Allafchian, "Magnetic solid-phase extraction to preconcentrate ultra trace amounts of lead(ii) using modified-carbon nanotubes decorated with NiFe2O 4 magnetic nanoparticles," *Anal. Methods*, vol. 5, no. 16, pp. 3903–3908, 2013.

[16] B. Ali *et al.*, "Preparation of Carbon Nanotubes via Chemical Technique (Modified Staudenmaier Method)," *Nanosci. &Nanotechnology-Asia*, vol. 7, no. 1, pp. 113–122, 2017.

[17] F. Esterification, "Modification and functionalization of multiwalled carbon nanotube (MWCNT) via related papers," vol. 35, 2010.

[18] L. Thi Mai Hoa, "Characterization of multi-walled carbon nanotubes functionalized by a mixture of HNO3/H2SO4," *Diam. Relat. Mater.*, vol. 89, pp. 43–51, 2018.

[19] Z. A. Abdulnabi, "Synthesis and Characterization of some Selenazone Complexes and Nanoadsorbent Surfaces from Industrial Waste for Removing some Carcinogenic Dyes and Heavy Metals from Water," University of Basrah, 2021.

[20] H. Mohammadi, E. Nekobahr, J. Akhtari, M. Saeedi, J. Akbari, and F. Fathi, "Synthesis and characterization of magnetite nanoparticles by co-precipitation method coated with biocompatible compounds and evaluation of in-vitro cytotoxicity," *Toxicol. Reports*, vol. 8, pp. 331–336, 2021.

[21] X. J. Fan and X. Li, "Preparation and magnetic properties of multiwalled carbon nanotubes decorated by Fe3O4 nanoparticles," *Xinxing Tan Cailiao/New Carbon Mater.*, vol. 27, no. 2, pp. 111–116, 2012.

[22] F. R. P. Rocha, A. D. Batista, W. R. Melchert, and E. A. G. Zagatto, "Solid-phase extractions in flow analysis," *Anais da Academia Brasileira de Ciencias*, vol. 90, no. 1. pp. 803–824, 2018.

[23] T. N. Majid and A. A. Abdulwahid, "An effcient cheap source of activated carbon as solid phases for extraction and removal of Congo Red from aqueous solutions," *Anal. Methods Environ. Chem. J.*, vol. 5, pp. 40–54, 2022.

[24] A. A. Mizhir, H. S. Al-Lami, and A. A. Abdulwahid, "Kinetic, Isotherm, and Thermodynamic Study of Bismarck Brown Dye Adsorption onto Graphene Oxide and Graphene Oxide-Grafted-Poly (n-butyl methacrylate-co-methacrylic Acid)," *Baghdad Sci. J.*, vol. 19, pp. 132–140, 2022.

[25] G. Z. Kyzas and N. K. Lazaridis, "Reactive and basic dyes removal by sorption onto chitosan derivatives," *J. Colloid Interface Sci.*, vol. 331, pp. 32–39, 2009.

[26] Z. Bekçi, C. Özveri, Y. Seki, and K. Yurdakoç, "Sorption of malachite green on chitosan bead," *J. Hazard. Mater.*, vol. 154, no. 1–3, pp. 254–261, 2008.

[27] G. Z. Kyzas, D. N. Bikiaris, and N. K. Lazaridis, "Low-swelling chitosan derivatives as biosorbents for basic dyes," *Langmuir*, vol. 24, no. 9, pp. 4791–4799, 2008.

[28] M. Hossein, N. Dalali, A. Karimi, and K. Dastanra, "Solid phase extraction of copper, nickel, and cobalt in water samples after extraction using surfactant coated alumina modified with indane-1, 2, 3-trione 1, 2-dioxime and determination by flame atomic absorption spectrometry," *Turkish Journal of Chemistry*, vol. 34, no. 5. pp. 805–814, 2010.

[29] A. A. Gouda and W. A. Zordok, "Solid-phase extraction method for preconcentration of cadmium and

lead in environmental samples using multiwalled carbon nanotubes," *Turkish J. Chem.*, vol. 42, no. 4, pp. 1018–1031, 2018.

[30] S. M. Sorouraddin, M. R. Afshar Mogaddam, M. R. A. Mogaddam, and M. R. Afshar Mogaddam, "Development of molecularly imprinted-solid phase extraction combined with dispersive liquid–liquid microextraction for selective extraction and preconcentration of triazine herbicides from aqueous samples," *Iran. Chem. Soc.*, vol. 13, no. 6, pp. 1–12, 2016.

[31] H. A. Mashayekhi and F. Khalilian, "Development of Solid-Phase Extraction Coupled with Dispersive Liquid-Liquid Microextraction Method for the Simultaneous Determination of Three Benzodiazepines in Human Urine and Plasma," *J. Chromatogr. Sci.*, vol. 54, no. 6, pp. 1068–1073, 2016.

[32] J. L. L. Urraca, M. Castellari, C. A. A. Barrios, and M. C. C. Moreno-Bondi, "Multiresidue analysis of fluoroquinolone antimicrobials in chicken meat by molecularly imprinted solid-phase extraction and high performance liquid chromatography," *J. Chromatogr. A*, vol. 1343, pp. 1–9, 2014.

[33] L. R. Snyder, "Classification off the solvent properties of common liquids," *J. Chromatogr. Sci.*, vol. 16, no. 6, pp. 223–234, 1978.

[34] T. S. Anokhina, A. A. Yushkin, P. M. Budd, and A. V. Volkov, "Application of PIM-1 for solvent swing adsorption and solvent recovery by nanofiltration," *Sep. Purif. Technol.*, pp. 1–8, 2015.

[35] G. Daneshvar Tarigh and F. Shemirani, *Simultaneous in situ derivatization and ultrasound-assisted dispersive magnetic solid phase extraction for thiamine determination by spectrofluorimetry*, vol. 123, no. October. Elsevier, 2014, pp. 71–77.

[36] E. Yilmaz, G. Guzel Kaya, and H. Deveci, "Removal of methylene blue dye from aqueous solution by semi-interpenetrating polymer network hybrid hydrogel: Optimization through Taguchi method," *Journal of Polymer Science, Part A: Polymer Chemistry*, vol. 57, no. 10. pp. 1070–1078, 2019.

[37] I. Langmuir, "The constitution and fundamental properties of solids and liquids. Part II.-Liquids," *Journal of the Franklin Institute*, vol. 184, no. 5. p. 721, 1917.

[38] J. Wang, Y. Ji, S. Ding, H. Ma, and X. Han, "Adsorption and desorption behavior of tannic acid in aqueous solution on polyaniline adsorbent," *Chinese Journal of Chemical Engineering*, vol. 21, no. 6. pp. 594–599, 2013.

[39] M. Erdem, E. Yüksel, T. Tay, Y. Çimen, and H. Türk, "Synthesis of novel methacrylate based adsorbents and their sorptive properties towards p-nitrophenol from aqueous solutions," *Journal of Colloid and Interface Science*, vol. 333, no. 1. pp. 40–48, 2009.

[40] M. K. Al Temimi and M. Erdem, "Adsorption of Reactive Black 5 dye onto two kinds of Poly (vinyl imidazole) in aqueous solutions.," *J. Basrah Res.*, vol. 41, pp. 145–157, 2015.

[41] D. Kurniawati, Y. Prestica, S. Sy, and N. L. Pernadi, "Methylene blue adsorption by langsat peel (*Lansium domesticum*) waste" *J. Litbang Ind.*, vol. 13, pp. 93 – 98, 2023.